ORIGINAL RESEARCH

Reversal of multidrug resistance in MCF-7/Adr cells by codelivery of doxorubicin and BCL2 siRNA using a folic acid-conjugated polyethylenimine hydroxypropyl-β-cyclodextrin nanocarrier

Jin-Ming Li
Wei Zhang
Hua Su
Yuan-Yuan Wang
Cai-Ping Tan
Liang-Nian Ji
Zong-Wan Mao

MOE Key Laboratory of Bioinorganic and Synthetic Chemistry, School of Chemistry and Chemical Engineering, Sun Yat-sen University, Guangzhou, People's Republic of China

Abstract: Systemic administration of chemotherapy for cancer often faces drug resistance, limiting its applications in cancer therapy. In this study, we developed a simple multifunctional nanocarrier based on polyethylenimine (PEI) to codeliver doxorubicin (DOX) and BCL2 small interfering RNA (siRNA) for overcoming multidrug resistance (MDR) and enhancing apoptosis in MCF-7/Adr cancer cells by combining chemotherapy and RNA interference (RNAi) therapy. The low-molecular-weight branch PEI was used to conjugate hydroxypropyl-β-cyclodextrin (HP-β-CD) and folic acid (FA), forming the codelivery nanocarrier (FA-HP-β-CD-PEI) to encapsulate DOX with the cavity HP-β-CD and bind siRNA with the positive charge of PEI for tumor-targeting codelivering drugs. The drug-loaded nanocomplexes (FA-HP-β-CD-PEI/DOX/siRNA) showed uniform size distribution, high cellular uptake, and significant gene suppression of BCL2, displaying the potential of overcoming MDR for enhancing the effect of anticancer drugs. Furthermore, the nanocomplexes achieved significant cell apoptosis through a mechanism of downregulating the antiapoptotic protein BCL2, resulted in improving therapeutic efficacy of the coadministered DOX by tumor targeting and RNA interference. Our study indicated that combined RNAi therapy and chemotherapy using our functional codelivery nanocarrier could overcome MDR and enhance apoptosis in MDR cancer cells for a potential application in treating MDR cancers.

Keywords: tumor targeting, codelivery, doxorubicin, BCL2 siRNA, overcome multidrug resistance

Introduction

Cancer is one of the major causes of death in the world, and the incidence of cancer continues to increase at an alarming rate.[1] Currently, chemotherapy remains a commonly used therapeutic approach for many cancers. Indeed, chemotherapy is relatively effective for the treatment of certain cancers, and it may be the only therapy that is appropriate for certain cancers. However, a common problem with chemotherapy is the development of multidrug resistance (MDR).[2] Usually, the MDR can be divided into two distinct classes based upon the mechanism used: protein pump dependent and protein pump-independent resistance.[3] The main mechanism of pump-independent resistance is the activation of a cellular antiapoptotic defense process, which involves the upregulation of the *BCL2* gene. Most clinically used anticancer drugs, which aim to trigger apoptosis, simultaneously activate both pump-, and non-pump-dependent cellular defenses over the duration of chemotherapy, which is longer than desired due

Correspondence: Zong-Wan Mao
MOE Key Laboratory of Bioinorganic and Synthetic Chemistry, School of Chemistry and Chemical Engineering, Sun Yat-sen University, Guangzhou, Guangdong 510275, People's Republic of China
Tel +86 20 8411 3788
Fax +86 20 8411 2245
Email cesmzw@mail.sysu.edu.cn

to dose limitations, ultimately rendering the treatment ineffective. Therefore, it is apparent that to efficiently suppress the overall resistance to chemotherapy, an important method to suppress therapeutic resistance is through the use of inhibitors that target the mechanism of resistance, such as inhibiting the expression of MDR1 or BCL2.[4]

RNA interference (RNAi) has emerged as an attractive technology for silencing the expression of specific genes in human cells.[5] In the physiological RNAi pathway of gene silencing, double-stranded RNAs are processed into small interfering RNAs (siRNAs) by the RNase enzyme Dicer. Nanocarriers represent particularly attractive delivery systems for siRNA, and may provide the foundation for rational design and formulation of RNAi-triggering nanomedicines.[6–8] siRNA can be delivered with a therapeutic intent using biomaterial-based delivery platforms, such as polymers,[9–11] liposomes,[12,13] chitosan,[14,15] and quantum dots,[16,17] among others. Therefore, the various available therapies would be much more effective at much lower doses if siRNA against the therapeutic resistance could be identified and successfully codelivered by nanocarriers, such as polymer conjugates,[18] micelles,[19] liposomes,[20] meso porous silica nanoparticles,[21] gold nanorods,[22] and quantum dots.[23] Although these codelivery systems have shown great success in resistance cancer-therapy research, a simple-preparation, low-cost, safe, highly transfection-efficient, and tumor-targeted codelivery vector system is still desired in current medical practice.

Polyethylenimine (PEI) is a cationic polymer often used in nonviral gene transfer, which can provide for efficient, in vitro gene transfer, and this efficiency is speculated to be at least partially due to enhanced endosome escape via pH buffering.[24] PEI is considered the most potent and promising alternative carrier, providing stable nucleic acid nanoparticles and exhibiting a unique "proton-sponge effect" for endosomal release of the nanoparticles into cytosol when it was first used for gene delivery in 1995.[25] Nevertheless, the use of PEI as an in vitro and in vivo transfection reagent is severely limited by its toxicity and difficulties in formulation.[26] Low-molecular-weight (LMW) PEI, on the other hand, was less toxic, but showed rather poor transfection activity.[27] To overcome this dilemma, one effective approach is to cross-link LMW PEI to form high-molecular-weight conjugates via stimuli-responsive linkage. While their toxicity is still low, these cross-linked conjugates showed considerably high transfection efficiency.[28] Another common strategy is to introduce a biocompatible or biodegradable polymer backbone/core to assemble LMW PEI, such as conjugating LMW PEI with cyclodextrin (CD) to form star-shaped copolymers.[29,30]

CDs are cup-shaped molecules that have a hydrophobic cavity and a hydrophilic exterior, and have the ability to interact with various hydrophobic guest molecules to form supramolecular inclusion complexes.[31] CD has been exploited to enhance the bioavailability of insoluble drugs by increasing the drug solubility, dissolution, and drug permeability.[32] Therefore, the safety of CD in humans is well established and clear. Among CDs, hydroxypropyl-β-CD (HP-β-CD) has been widely used in pharmaceutical applications and supramolecular research because of its ready availability and cavity size suitable for the widest range of drugs or guest molecules, and has been approved by FDA.[33–35] Based on these reasons, many classes of linear, water-soluble CD-containing polymers have been developed and intensively studied both in vitro and in vivo for drug delivery.[36–38] These studies have shown that CDs possess significant biocompatibility, and are capable of delivering not only small molecular drugs but also nucleic acid, such as DNA and siRNA efficiently.

In addition to modifying and optimizing the polymeric gene-carrier backbones, different target-specific ligands, including various signal-transduction proteins (antibodies) and small molecules, have also been explored to promote target-specific gene delivery in vitro and in vivo.[39] Folic acid (FA) in particular has been found to be an optimal ligand for targeting tumor cells, due to its low immunogenicity, low toxicity, and high affinity to the folate receptor, which overexpresses in certain cancer cells.[40]

We developed a simple multifunctional codelivery nanocarrier (FA-HP-β-CD-PEI) to tumor-targeted codelivery of DOX and BCL2 siRNA for reversal of drug resistance and enhancing MCF-7/Adr cancer cell apoptosis (Figure 1). In this study, the HP-β-CD was cross-linked with LMW branch PEI first to decrease the cytotoxicity and keep high cell transfection of nanocarriers. Then, the FA was conjugated with HP-β-CD-PEI to form a copolymer as the codelivery nanocarrier that could encapsulate DOX with the cavity of HP-β-CD and bind siRNA with positively charged PEI for tumor-targeted delivering drugs. With this design, the FA-HP-β-CD-PEI nanocarrier showed good water-solubility and biocompatibility, resulting in the coloaded drug nanocomplexes achieving uniform size distribution and high cell transfection, with commendable gene silencing and satisfactory cell apoptosis, suggesting the potential of using this codelivery nanocarrier to overcome MDR and improve chemotherapy by combining siRNA-mediated gene
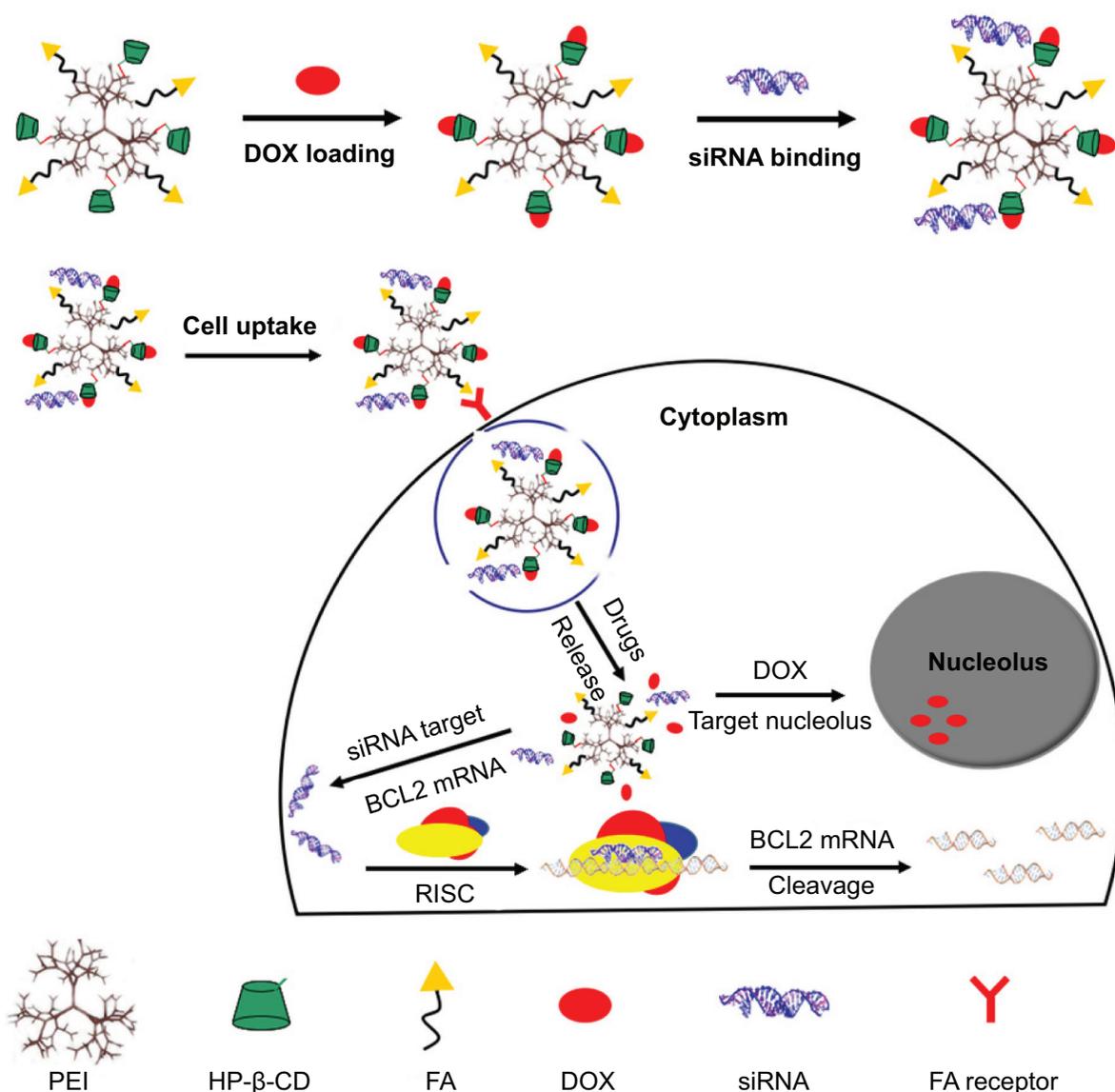
Figure 1 Schematic representation of DOX loading and BCL2 siRNA binding with the tumor targeting co-delivery nanocarrier (FA-HP-β-CD-PEI) for forming nanocomplexes to overcome MDR and enhance apoptosis in MCF-7/Adr tumor cells.
Abbreviations: DOX, doxorubicin; siRNA, small interfering RNA; mRNA, messenger RNA; MDR, multidrug resistance; FA, folic acid; HP-β-CD, hydroxypropyl-β-cyclodextrin; PEI, polyethylenimine; RISC, RNA-induced silencing complex.

silencing and tumor targeting. We expect this codelivery nanocarrier can significantly enhance therapeutic efficacy against drug resistance in MDR cancer therapy.

Materials and methods
Materials and reagents

PEI, MW 600 Da and 25 kDa, HP-β-CD, FA, 1,1-carbonyl-diimidazole (CDI), dicyclohexylcarbodiimide (DCC), *N*-hydroxysuccinimide (NHS), 3-(4,5-dimethyl-thiazol-2-yl)-2, 5-diphenyl tetrazolium bromide (MTT), and Hoechst 33258 were obtained from Sigma-Aldrich (St Louis, MO, USA) and used without additional purification. Drug-fast

MCF-7/Adr cells (resistant to 1 μg/mL DOX) were obtained from Kaiji Biology (Nanjing, People's Republic of China [PRC]). The cells were routinely grown at 37°C in a humidified atmosphere with 5% CO_2 (in air) in 25 cm^2 culture flasks (Corning, New York, NY, USA) with Dulbecco's Modified Eagle's Medium (HyClone, Logan, UT, USA), and 10% fetal bovine serum (HyClone) and 1% penicillin streptomycin solution (HyClone) were added to the medium for optimal growth. The BCL2 siRNA duplexes were provided by Genpharm (Shanghai, PRC), and the sequences were 5′-AAGGC-CACAATCCTCCCCCAGCCTGTCTC-3′ and (anti-sense) 5′-AACTGGGGGAG-GATTGTGGCCCCTGTCTC-3′.

Other siRNA, including siRNA[FAM] (siRNA link with FAM green fluorescent dye) were also provided by Genpharm. The anti-BCL2 monoclonal antibody and β-actin monoclonal antibody were obtained from Abgent (San Diego, CA, USA).

Synthesis of FA-HP-β-CD-PEI

The FA-HP-β-CD-PEI nanocarriers were synthesized as per a previous report.[11] Briefly, 0.51 g (0.37 mmol) of HP-β-CD was dissolved in 6 mL of dimethyl sulfoxide (DMSO) and mixed with 0.49 g (3 mmol) of CDI (dissolved in 6 mL DMSO) with sufficient mixing. Next, 0.1 mL of triethylamine (Et₃N) was added to the mixture and stirred for 3 hours in the dark at room temperature. The hydroxyl group of HP-β-CD was activated by CDI and generated the HP-β-CD-CDI. This mixture was precipitated in cold ethyl ether, filtered, dissolved in 6 mL DMSO and stored at 4°C. A total of 1.8 g (3 mmol) of PEI 600 Da was dissolved in 6 mL DMSO. The previously prepared HP-β-CD-CDI in 6 mL DMSO and 0.1 mL Et₃N was added dropwise over 2 hours. It was further stirred for 6 hours, and the mixture was dialyzed with a dialysis tube (MW 2,000) for 2 days in running water. The final solution was lyophilized for 3 days to get the product (HP-β-CD-PEI).

The FA was conjugated with HP-β-CD-PEI by condensation reaction with DCC and NHS. Briefly, a total of 10 mg (0.023 mmol) FA was dissolved in 6 mL of DMSO with 9.5 mg (0.046 mmol) of DCC added to it. In another tube, 5.5 mg (0.046 mmol) of NHS was dissolved in 1.5 mL of DMSO, and this final solution was added to the FA solution made previously. Finally, 0.1 mL of Et₃N was added to activate the FA. This was followed by dissolving 120 mg of HP-β-CD-PEI in 6 mL DMSO. The described activated FA solution was added dropwise over 2 hours. It was further stirred for 6 hours in order to cross-link the carboxyl residue of the FA with the amino groups of PEI. The final solution was dialyzed using a dialysis tube (MW 2,000) for 2 days in running-water. The final solution was lyophilized for 3 days to get the final product (FA-HP-β-CD-PEI). By this synthesis method, we got about 115 mg FA-HP-β-CD-PEI in one reaction.

Preparation and characterization of FA-HP-β-CD-PEI/DOX nanocomplexes

Five milligrams of FA-HP-β-CD-PEI was mixed in a 5 mL DOX solution (phosphate-buffered saline [PBS], 0.5 mg/mL), followed by ultrasonic agitation in a type 60 Sonic Dismembrator (Fisher Scientific, Waltham, MA, USA) for 24 hours.

Centrifugation was conducted to collect the FA-HP-β-CD-PEI/DOX nanocomplexes. The supernatant solution was collected and measured by an ultraviolet (UV)-visible spectrophotometer (Cary 300; Varian Medical Systems, Palo Alto, CA, USA) to quantify indirectly how many DOX were encapsulated with the FA-HP-β-CD-PEI nanocarrier (DOX-entrapment efficiency). The formation of FA-HP-β-CD-PEI/DOX nanocomplexes was confirmed by Fourier-transform infrared (FTIR; Bruker, Karlsruhe, Germany) and ¹H nuclear magnetic resonance (NMR) spectroscopy (300 MHz AV 300; Bruker). The size of nanocomplexes was measured by transmission electron microscopy (TEM; JEOL, Tokyo, Japan) and dynamic light scattering (DLS; zeta-potential analyzer, Beckman Coulter, Brea, CA, USA). Zeta potential was measured by a zeta-potential analyzer (Beckman Coulter).

Preparation and characterization of FA-HP-β-CD-PEI/DOX/siRNA nanocomplexes

The FA-HP-β-CD-PEI/DOX/siRNA nanocomplexes were prepared as described. In short, FA-HP-β-CD-PEI/DOX nanocomplexes were incubated with siRNA at room temperature for 1 hour to form the FA-HP-β-CD-PEI/DOX/siRNA nanocomplexes. The N/P ratio between the siRNA and FA-HP-β-CD-PEI/DOX nanocomplexes was varied from 0 to 32 by gel electrophoresis to achieve the optimal N/P ratio for the following experiments. The naked siRNA and FA-HP-β-CD-PEI/DOX/siRNA nanocomplexes were loaded in wells of 1.5% agarose gel with 150 V for 10 minutes. Because of the siRNA[FAM], gel imaging could be undertaken directly with the fluorescent gel-imaging system (Alpha Innotech, San Leandro, CA, USA) with excitation (Ex) 488 nm and emission (Em) 532 nm. The size of FA-HP-β-CD-PEI/DOX/siRNA nanocomplexes was measured by TEM and DLS.

In vitro DOX-release assay at different pH

To investigate DOX-release behavior in vitro, FA-HP-β-CD-PEI/DOX nanocomplexes were incubated in PBS at different pH (7.4 and 5.0) at 37°C for different times (0–48 hours), and then transferred into a dialysis bag (MW cutoff 14,000 Da). The bag was placed into the same buffered solution (50 mL), and then the solution was measured with UV-visible spectrophotometry at different time points (0, 6, 12, 24, and 48 hours) to quantify how much DOX was released from the carrier.

Cell transfection

The cellular uptake of nanocomplexes was verified by confocal scanning laser microscopy (CSLM; TCS SP5; Leica, Wetzlar, Germany) and flow cytometry (FCM; FACSCalibur™; BD Biosciences, San Jose, CA, USA). For confocal imaging, MCF-7/Adr cells were seeded in a laser confocal microscopy 35 mm² petri dish (MatTek, Ashland, MA, USA) at a density of 10^5 cells for 24 hours. The media containing serum were added into the solution, and cells were incubated with HP-β-CD-PEI/DOX/siRNA[FAM], FA-HP-β-CD-PEI/DOX/siRNA[FAM], and FA + FA-HP-β-CD-PEI/DOX/siRNA[FAM] nanocomplexes for 4 hours; the free DOX (0.5 μg/mL) was used as a control. After transfection, the cells were washed with PBS and stained with Hoechst 33342 solutions: Hoechst 33342, Ex 405, Em 475; siRNA[FAM], Ex 488, Em 535; DOX, Ex 488, Em 585.

For FCM, the cells were seeded in a six-well plate at 10^6/well, and then incubated with nanocomplexes for 4 hours; the free DOX (0.5 μg/mL) was as a control. After transfection, the cells were washed with PBS three times. The pancreatin (Invitrogen, New York, NY, USA) was used to digest cells, and cells were collected by centrifugation. We used a 488 nm laser for siRNA[FAM] and DOX excitation to analyze cells in each group. The fluorescence from DOX was collected through a 585 nm filter, and the green emission of FAM was measured with a 535 nm filter. Normally cultured cells without nanocomplex transfection were used as a control for background calibration.

Western blot

After transfection with nanocomplexes, the treatment cells were lysed using M-PER® protein-extraction reagent (Pierce, Rockford, IL, USA). The untreated cells were used as a control. The lysates were separated by centrifugation at 12,000 rpm at 4°C for 10 minutes on a 5417R centrifuge (Eppendorf, Hamburg, Germany). Supernatants were then collected, and the protein concentration was measured by a standard bicinchoninic acid protein-assay kit (Novagen, Madison, WI, USA). Equal amounts of protein were loaded and separated on 12% sodium dodecyl sulfate polyacrylamide gel electrophoresis, and then were transferred for 1 hour at 150 V using a Mini-Protean4 (Bio-Rad, Philadelphia, PA, USA) to nitrocellulose membranes (Bio-Rad) in transfer buffer (25 mM Tris HCl, 200 mM glycine, 10% methanol) and blocked with 5% milk blocking buffer for 2 hours on a horizontal shaker. The blocked membranes were incubated with 1:1,000 VEGF mouse monoclonal antibodies diluted in 5% milk blocking buffer. The membranes were washed in Tween–Tris buffered

saline (0.1% Tween-20 in 100 mM Tris HCl [pH 7.5], 0.9% NaCl) and probed with horseradish peroxidase-linked labeled mouse antirabbit secondary antibodies diluted at 1:5,000 in 5% milk blocking buffer. The blots were developed by using an enhanced chemiluminescence kit (Amersham, New York, NY, USA). The membranes were exposed to Kodak X-OMAT film for 10–30 seconds for data acquisition and developed using a conventional film-developing machine.

Evaluation of cytotoxicity and apoptosis in MCF-7/Adr cells by MTT and FCM

For the MTT assay, the cells were collected by trypsinization, counted, and plated in 96-well flat-bottomed microtiter plates at a density of 5,000 cells per well, with 100 μL of cell-suspension medium per well. In the cytotoxicity study, the free DOX and nanocomplexes were added and incubated with cells for 48 hours. The cells were then incubated with 20 μL of MTT for 4 hours at 37°C, and then the medium was sponged up and 100 μL DMSO added to dissolve the crystals. The Infinite F200 device (Tecan, Männedorf, Switzerland) at a wavelength of 595 nm was used to analyze the absorbance. The relative cell growth (%) for the controls (containing cell-culture medium) was calculated as: test/control ×100.

For FCM, the cytotoxicity induced by free DOX (0.5 μg/mL), HP-β-CD-PEI/DOX, HP-β-CD-PEI/siRNA, HP-β-CD-PEI/DOX/siRNA, FA-HP-β-CD-PEI/DOX, FA-HP-β-CD-PEI/siRNA, and FA-HP-β-CD-PEI/DOX/siRNA nanocomplexes were assayed by FCM with an annexin V/propidium iodide (PI) kit (Invitrogen) to assess apoptosis levels induced after 48 hours. Treated MCF-7/Adr cells were harvested and stained with fluorescein isothiocyanate (FITC)-annexin V at room temperature for 10 minutes, followed by a PI working solution at 0°C for 15 minutes prior to measurements via FCM. The cells were analyzed in each group with Ex 488 for FITC and PI, Em 535 for FITC, and Em 615 for PI.

Observing MCF-7/Adr cell-apoptosis morphology by Bio-TEM

To observe the apoptosis morphology of MCF-7/Adr cells after transfection with nanocomplexes, the treated MCF-7/Adr cells were collected and fixed, and were then frozen and made into sections. The cell section was stuck on the copper online surface and observed by TEM.

Statistical analysis

Statistical analysis was performed using SPSS software (version 17.0; SPSS Inc., Chicago, IL, USA). Results are reported as mean ± standard deviation. Statistical significance among

groups was determined by one-way analysis of variance with Bonferroni correction. Probability values of $P<0.05$ were considered significant.

Results and discussion
Preparation and characterization of DOX-loaded nanocomplexes

The DOX-loaded nanocomplexes (FA-HP-β-CD-PEI/DOX) were prepared by sonic oscillation. The appropriate amount of FA-HP-β-CD-PEI and DOX was mixed together, then an oscillator was used to sonically oscillate the mixture overnight to achieve the DOX-loaded nanocomplexes. The mixture was centrifuged to collect the FA-HP-β-CD-PEI/DOX nanocomplexes. The supernatant solution was also collected to quantify the remaining concentration of DOX by UV-visible spectrophotometry, and then the quantity of DOX loaded in FA-HP-β-CD-PEI nanocarriers was ascertained. Table S1 shows the loading content of DOX with the nanocarrier. The formation of FA-HP-β-CD-PEI/DOX nanocomplexes was characterized by FTIR and ^{1}H NMR spectroscopy, as shown in Figures S1 and S2. In Figure S1A, the characteristic absorption of free DOX appeared at 1,900–800 cm^{-1}; these peaks represent the characteristic absorption of the anthracene nucleus and molecular bone vibration of DOX, especially the peak of 1,795 cm^{-1}. The characteristic absorption of the FA-HP-β-CD-PEI carrier appeared at 1,630–800 cm^{-1} and 3,400–3,200 cm^{-1} (Figure S1B); these peaks showed characteristic absorption of the bone structure and O–H vibration sorption of PEI and HP-β-CD, especially the peak of 2,915 cm^{-1}. When it comes to Figure S1C, the FTIR spectrogram is different: the peak of FA-HP-β-CD-PEI/DOX nanocomplexes was 1,795 cm^{-1}, which is similar with free DOX, meaning the nanocomplexes contained DOX. But the intensity of peaks at 1,700–1,200 cm^{-1} was changed (became blunt), and especially the characteristic absorption of C=O, displaying the characteristic absorption of the anthracene nucleus in the DOX, was reduced. These reductions showed that the anthracene nucleus of DOX was encapsulated in the cavity of HP-β-CD and caused vibration and the form of FA-HP-β-CD-PEI/DOX complex limit the shock of DOX.

Next, we characterized the formation of FA-HP-β-CD-PEI/DOX nanocomplexes by ^{1}H NMR (Figure S2). Figure S2, A and B show the ^{1}H NMR of free DOX and FA-HP-β-CD-PEI nanocarriers, respectively. When it comes to Figure S2C, the ^{1}H NMR of FA-HP-β-CD-PEI/DOX nanocomplexes contained the ^{1}H peak of 3.56 ppm, which was similar with Figure S2A (free DOX), indicating the nanocomplexes

contained DOX, but compared with Figure S2B, the ^{1}H NMR of FA-HP-β-CD-PEI/DOX nanocomplexes moved to a low field (^{1}H position: 1.038 ppm, CH$_3$ of hydroxypropyl; 2.4–3.0 ppm, CH$_2$ of PEI), showing the anthracene nucleus of the free DOX inserted into the cavity of HP-β-CD changed the shape of the cavity, demonstrating the formation of FA-HP-β-CD-PEI/DOX nanocomplexes.

Preparation and optimization of DOX- and siRNA-coloaded nanocomplexes

After successful preparation of the FA-HP-β-CD-PEI/DOX nanocomplexes, BCL2 siRNA was added to prepare FA-HP-β-CD-PEI/DOX/siRNA nanocomplexes. Through electrostatic interaction, siRNA could adsorb with the positive FA-HP-β-CD-PEI carrier. To find out the optimized ratio of FA-HP-β-CD-PEI/DOX:siRNA, we used gel electrophoresis to test the behavior of FA-HP-β-CD-PEI/DOX/siRNA nanocomplexes with the agarose gel. As shown in Figure 2, in different N/P ratio of FA-HP-β-CD-PEI/DOX:siRNA (0, 1, 2, 4, 8, 16, 32), the siRNA was retarded gradually by FA-HP-β-CD-PEI/DOX nanocomplexes. When the N/P ratio was 16:1, the siRNA was retarded completely in the hole, showing this N/P ratio was appropriate to bind siRNA for the following experiments. Although the N/P ratio of 32:1 got the higher zeta potential (Table S1) for higher cell transfection, considering about the balance of cell transfection and cytotoxicity, we chose the N/P ratio of 16:1 for the following experiments.
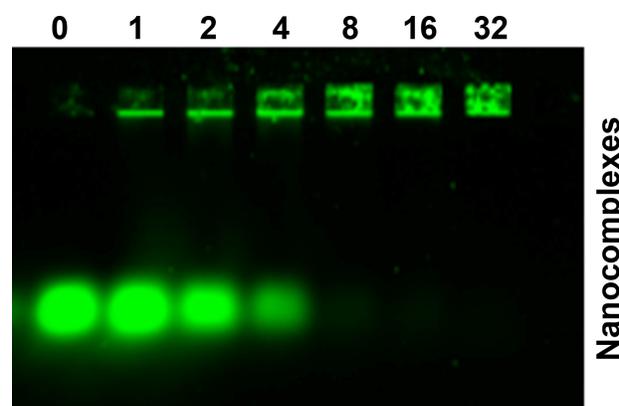

Figure 2 Characterization of FA-HP-β-CD-PEI/DOX/siRNA^{FAM} nanocomplexes by gel electrophoresis assay.
Notes: The agarose gel electrophoresis showed the behavior of nanocomplexes with various N/P ratios (0, 1, 2, 4, 8, 16, and 32). When the N/P ratio was 16:1, the siRNA was retarded completely, and this N/P ratio was used in the following experiments. siRNA^{FAM} Ex =488 nm, Em =535 nm, and the concentration was 100 nM. The gel was 1.5% and run for 10 minutes at 150 V.
Abbreviations: DOX, doxorubicin; siRNA^{FAM}, small interfering RNA link with FAM green fluorescent dye; FA, folic acid; HP-β-CD, hydroxypropyl-β-cyclodextrin; PEI, polyethylenimine; Ex, excitation; Em, emission.

Characterization of drug-loaded nanocomplexes

The size of drug-loaded nanocomplexes was measured by TEM and DLS, as shown in Figure 3. From TEM imaging, the FA-HP-β-CD-PEI/DOX nanocomplexes (Figure 3A) and FA-HP-β-CD-PEI/DOX/siRNA nanocomplexes (Figure 3B) all showed good morphology and distribution. Interestingly, after adding siRNA, the FA-HP-β-CD-PEI/DOX/siRNA nanocomplexes became smaller (Table S1) and more compact. This change (smaller and more compact) will be an advantage for cell uptake. Furthermore, the size of the drug-loaded nanocomplexes also was measured by DLS (Figure 3C and D), showing the a similar result of uniform distribution of the nanocomplexes and size change of nanocomplexes after adding siRNA. It has been reported that polymeric nanoparticles of 100–200 nm in size acquire the best properties for escaping phagocytic uptake, and nanoparticles <300 nm are also suitable to use for cellular uptake and general transport.[41,42] However, larger nanoparticles (>300 nm) tend to be arrested by the reticuloendothelial system and trapping of hepatic sinusoid, which results in higher hepatic disposition.[43] For the FA-HP-β-CD-PEI/DOX/siRNA nanocomplexes, the size of the nanocomplexes was <300 nm (Figure 3B, Table S1), which should be suitable for using this nanocomplexes for tail-vein injection with systemic administration and to obtain efficient tumor accumulation by the FA tumor-targeted group.[11]

DOX-release behavior at different pH

For the study of the DOX-release behavior of FA-HP-β-CD-PEI/DOX nanocomplexes, a controlled-release experiment was performed (with two pH: 5.0 and 7.4). In Figure 4, compared to the release speed at pH 7.4, the DOX release from nanocomplexes was much faster at pH 5.0. The cause of this phenomenon lies in the low pH of acidic condition making the cavity of HP-β-CD change to let the DOX release from HP-β-CD more easily, and the DOX is more hydrophilic at low pH, making it release from the nanocarrier much faster.[44]
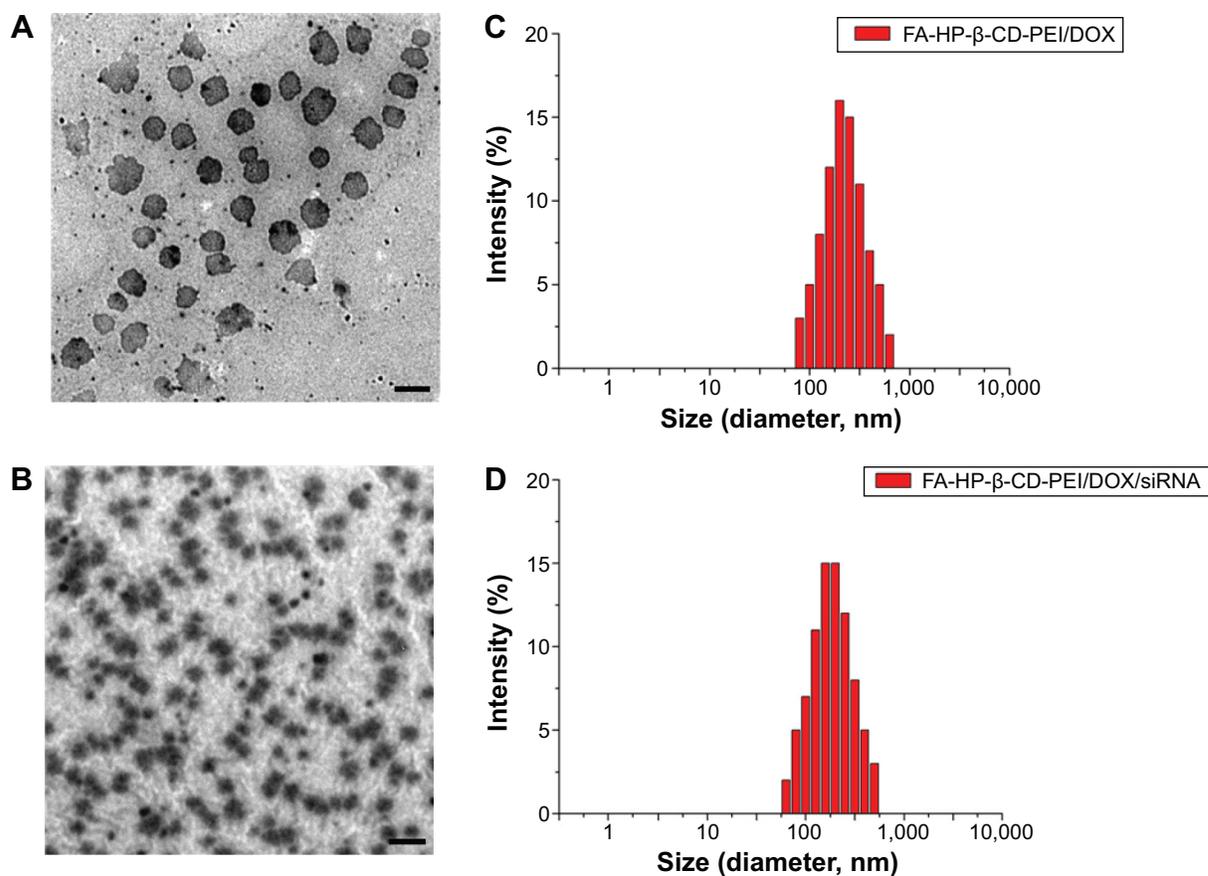

Figure 3 TEM images and DLS measure of drug-loaded nanocomplexes.
Notes: (**A**) TEM imaging of FA-HP-β-CD-PEI/DOX nanocomplexes; (**B**) TEM imaging of FA-HP-β-CD-PEI/DOX/siRNA nanocomplexes; (**C**) DLS of FA-HP-β-CD-PEI/DOX nanocomplexes; (**D**) DLS of FA-HP-β-CD-PEI/DOX/siRNA nanocomplexes. The N/P ratio was 16:1, and the concentration of siRNA was 100 nM. The scale bar 500 nm (**A**, **B**).
Abbreviations: TEM, transmission electron microscopy; DLS, dynamic light scattering; DOX, doxorubicin; siRNA, small interfering RNA; FA, folic acid; HP-β-CD, hydroxypropyl-β-cyclodextrin; PEI, polyethylenimine.
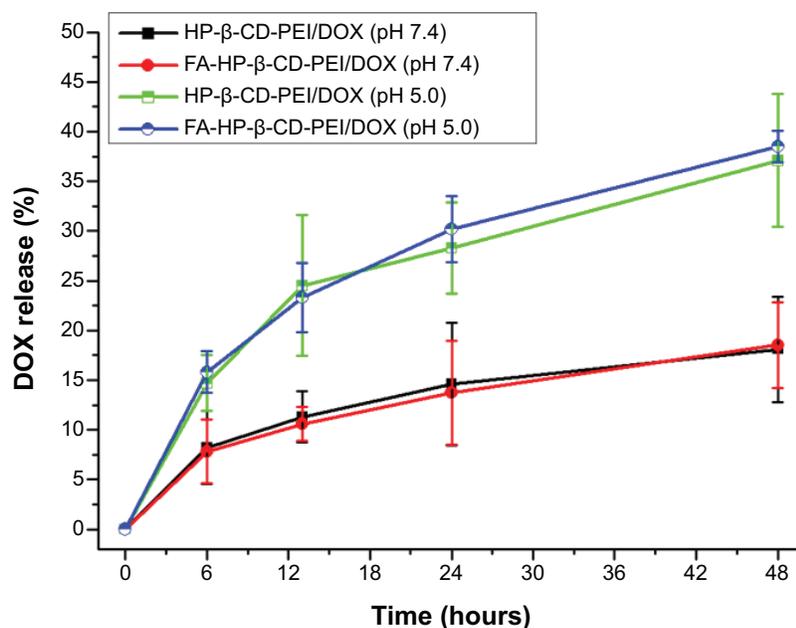
Figure 4 The release behavior of the DOX from the DOX-loaded nanocomplexes in different pH conditions (pH 5.0 and pH 7.4).
Notes: When the DOX-loaded nanocomplexes were in the normal pH condition (pH 7.4), the DOX released from the nanocomplexes very slowly, and compared to the normal pH condition, the DOX released very quickly at pH 5.0 from the nanocomplexes, showing that the release of the DOX from the nanocarrier can be controlled by pH. DOX concentration of 0.5 μg/mL.
Abbreviations: DOX, doxorubicin; siRNA, small interfering RNA; FA, folic acid; HP-β-CD, hydroxypropyl-β-cyclodextrin; PEI, polyethylenimine.

This characteristic is very meaningful, because when this nanocarrier is used to deliver DOX in vivo, DOX release from the nanocarrier is very little in normal conditions (pH 7.4). It is also very useful to reduce the loss of DOX in the delivery process for reducing the site effect of DOX at the same time. Moreover, this can increase the water-solubility of DOX and the cycle in vivo when using this nanocarrier to load DOX. When the drug-loaded nanocomplexes are delivered to the tumor, the tumor cells will uptake the nanocomplexes and form a lysosomal vesicle. In the lysosomal vesicle with low pH, the DOX will release from the nanocomplexes rapidly and target the nucleus of the tumor cells to kill them. We also performed the DOX release experiment with the FA-HP-β-CD-PEI/DOX/siRNA nanocomplexes and got a similar result, which showed that there was no effect on DOX-release behavior after siRNA binding (Figure S3).

Study on cell uptake

Cell-uptake efficiency of the FA-HP-β-CD-PEI/DOX/siRNA nanocomplexes was evaluated by CSLM and FCM. FAM-labeled scrambled siRNA was used to visualize the cell uptake of siRNA, and the red fluorescence of DOX was observed simultaneously. The free DOX and nontargeting HP-β-CD-PEI/DOX/siRNA nanocomplexes were used for comparison of cell-uptake efficiency. As shown in Figure 5, after 4 hours' incubation with MCF-7/Adr cells, the

FA-HP-β-CD-PEI/DOX/siRNA nanocomplexes showed much stronger green (siRNA[FAM]) and red (DOX) fluorescence, in comparison with nontargeting HP-β-CD-PEI/DOX/siRNA nanocomplexes (Figure 5A). This result showed that the FA-conjugated enhanced the cell uptake of the nanocomplexes greatly. When the cells were incubated with the free FA and FA-HP-β-CD-PEI/DOX/siRNA nanocomplexes simultaneously, the cell uptake of the FA-HP-β-CD-PEI/DOX nanocomplexes was affected and subdued, because the free FA could compete with the FA-HP-β-CD-PEI/DOX/siRNA nanocomplexes and decreased the cell uptake of FA-HP-β-CD-PEI/DOX/siRNA nanocomplexes, showing special tumor targeting of the nanocomplexes by FA. From the CSLM imaging, the result demonstrated that cross-linking the targeting group, such as FA, to the drug-delivery system could greatly increase the delivery efficiency of drugs and special tumor targeting in cancer therapy. The FCM measurement of positive (DOX and siRNA[FAM]) cells showed similar results (Figure 5B). Apparently, DOX and siRNA were much more efficiently transferred into cells using the targeting nanocomplexes rather than the nontargeting one and free DOX. Also, regardless of the difference in fluorescence intensities of DOX and siRNA, distributions of DOX-fluorescent cells and siRNA-fluorescent cells were identical in the low-magnification confocal images, and high-magnification confocal images further revealed
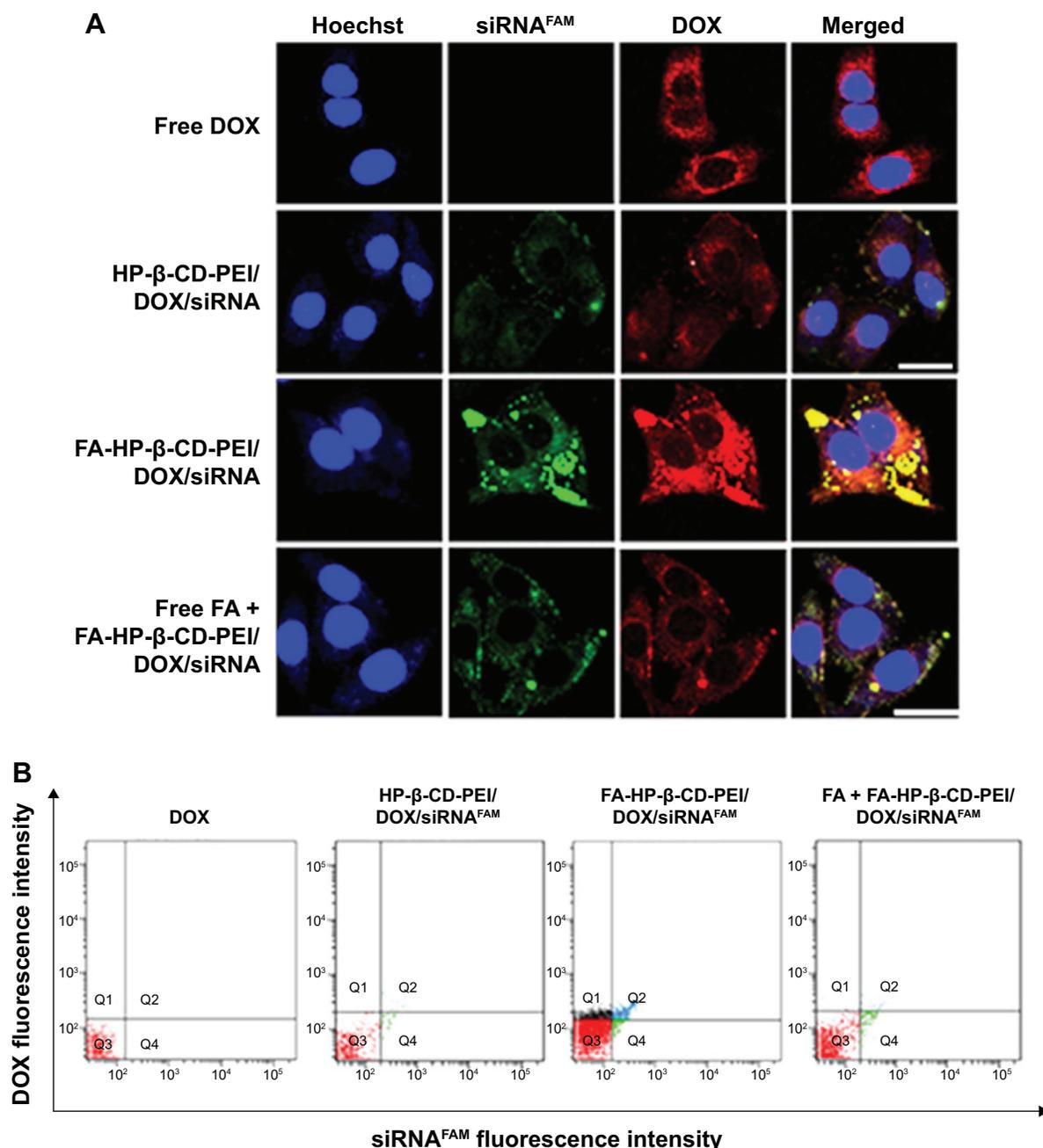
Figure 5 Cell uptake of FA-HP-β-CD-PEI/DOX/siRNA[FAM] nanocomplexes was evaluated by CSLM (**A**) and FCM (**B**) in MCF-7/Adr cells.
Notes: The free DOX, HP-β-CD-PEI/DOX/siRNA[FAM], and free FA + FA-HP-β-CD-PEI/DOX/siRNA[FAM] were used as contrast. The tumor-targeting nanocomplexes showed the strongest fluorescence in the experiments. Incubation time, 4 hours; siRNA, 100 nM; DOX, 0.5 μg/mL; blue, Hoechst 33342, Ex 405 nm, Em 435 nm; green, siRNA[FAM], Ex 488 nm, Em 535 nm; red, DOX, Ex 488 nm, Em 595 nm. Scale bars 40 μm (**A**).
Abbreviations: FA, folic acid; HP-β-CD, hydroxypropyl-β-cyclodextrin; PEI, polyethylenimine; DOX, doxorubicin; siRNA[FAM], small interfering RNA link with FAM green fluorescent dye; CSLM, confocal scanning laser microscopy; FCM, flow cytometry; Ex, excitation; Em, emission.

the identical intracellular distributions of DOX and siRNA fluorescence in the cytoplasm.

Suppression of *BCL2* gene expression
Chemical anticancer drugs, such as DOX, in the treatment of cancer are still the first choice for cancer therapy.

However, the application of chemical drugs is encountering an insurmountable bottleneck, due to the fact that cancer cells may develop several pathways to escape the apoptosis.[2,3] It is worthwhile noting that overcoming drug resistance by suppressing antiapoptotic genes is extremely meaningful in nanomedicine-mediated cancer chemotherapy, because

nanocarrier transportation of drugs can bypass the P-gp-mediated drug efflux from cells. This means that chemotherapy with multifunctional nanocomplexes containing anticancer drugs and siRNA that can target antiapoptotic genes may be used to solve this problem of the major drug-resistance pathways simultaneously. Among the antiapoptotic genes, the *BCL2* was found predominantly in the outer mitochondrial membrane, which can act effectively against cell apoptosis upon inhibiting the mitochondrial release of apoptosis-inducing factor and cytochrome C, which has been known to be a trigger for the caspase cascade in apoptosis.[45] Therefore, silencing the *BCL2* gene and suppressing the BCL2 protein by RNAi will be helpful for leading cancer-cell apoptosis and increasing the effect of chemical drugs (DOX).

Suppression of the expression of the *BCL2* gene in MCF-7/Adr cells was evaluated by protein levels in the present study by Western blot (WB). As shown in Figure 6, the untreated cells and naked siRNA were used as controls, and showed the highest expression of BCL2 protein ($100\% \pm 2.7\%$ and $97\% \pm 4.6\%$, respectively). We used two siRNA-transfection reagents (HiPerFect and siPort NeoFX) to compare with our nanocomplexes. From the WB result, the BCL2 protein expression of each treated group was: $36.3\% \pm 6.5\%$ (siPort NeoFX/siRNA), $43.5\% \pm 7.8\%$ (HiPerFect/siRNA), $30.4\% \pm 8.3\%$ (HP-β-CD-PEI/siRNA), $34.3\% \pm 4.7\%$ (HP-β-CD-PEI-DOX/siRNA), $8.8\% \pm 9.2\%$
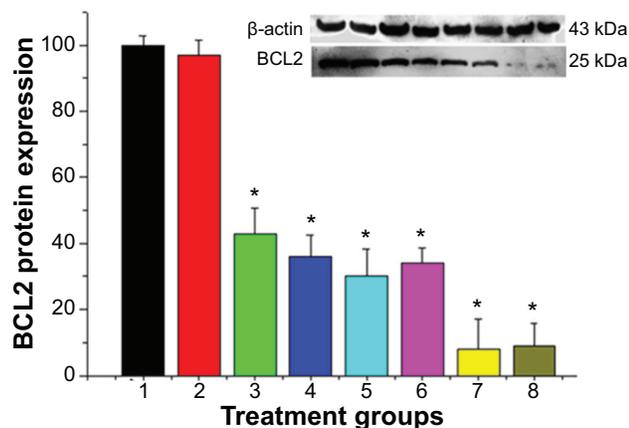

Figure 6 Western blot analysis showed the efficacy in suppressing BCL2 protein expression in MCF-7/Adr cells with different treatment groups (1, control; 2, naked siRNA; 3, HiPer-Fect/siRNA; 4, siPort NeoFX/siRNA; 5, HP-β-CD-PEI/siRNA; 6, HP-β-CD-PEI/DOX/siRNA; 7, FA-HP-β-CD-PEI/siRNA; 8, FA-HP-β-CD-PEI/DOX/siRNA).
Notes: The purchased siRNA reagents (HiPerFect from Qiagen, siPort NeoFX from Invitrogen) were used as the positive control. A significant difference was observed between control and different treatment groups. Data shown here are the mean ± standard deviation of three independent experiments. Incubation, 72 hours; siRNA concentration, 100 nM. *$P<0.05$ (n=3).
Abbreviations: siRNA, small interfering RNA; FA, folic acid; HP-β-CD, hydroxypropyl-β-cyclodextrin; PEI, polyethylenimine; DOX, doxorubicin.

(FA-HP-β-CD-PEI/siRNA), and $9.7\% \pm 6.9\%$ (FA-HP-β-CD-PEI/DOX/siRNA). Obviously, we achieved a high BCL2 protein-suppression efficiency with our nanocomplexes compared with the commercial siRNA-transfection reagents. Specially, the FA-HP-β-CD-PEI/siRNA nanocomplexes and FA-HP-β-CD-PEI/DOX/siRNA nanocomplexes achieved more than 90% BCL2 protein-suppression efficiency, and it is worth noting that this WB experiment was performed with FBS cells culture medium. More interestingly, compared with FA-HP-β-CD-PEI/siRNA nanocomplexes, the FA-HP-β-CD-PEI/DOX/siRNA nanocomplexes also achieved good BCL2 protein-suppression efficiency, showing that the FA-HP-β-CD-PEI nanocarrier still had very good ability to absorb, deliver, and release siRNA to silence the *BCL2* gene after encapsulating DOX. This high BCL2 protein suppression provided a good foundation for enhancing the effect of DOX and cell apoptosis.

Synergistic effects of siRNA and DOX on MCF-7/Adr cell apoptosis

Usually, the expression of *MDR1* and *BCL2* is at a high level in MDR cancer cells. If only DOX is used to treat MDR cancer cells for cell apoptosis, the MDR cancer cells will "pulse on" the mechanism of MDR and produce P-gp to pump the DOX outside the cells or highly express the *BCL2* gene to resist the apoptosis. This drug-resistance mechanism causes the curative effect of DOX to become very weak in cancer therapy. Silencing the *MDR1* gene or the *BCL2* gene by RNAi to increase the curative effect of DOX in cancer therapy is a good method to combat this drug-resistance mechanism, especially using nanocarriers to codeliver therapeutic siRNA and DOX for synergistic effects of siRNA and DOX on drug-resistant cell apoptosis. When the therapeutic siRNA silences the *BCL2* gene, it increases the curative effect of DOX and reduces the side effect of DOX by tumor-targeted delivery.

To verify the synergistic effect of siRNA and DOX by the codelivery nanocarriers, MTT assay and FCM were conducted to quantify cell apoptosis after 48 hours' treatment. From the MTT result (Figure 7), there was obvious cell apoptosis when using the drug-loaded nanocomplexes to treat the MCF-7/Adr cells compared to free DOX treatment (cell viability: free DOX, $94\% \pm 2.7\%$; HP-β-CD-PEI/DOX, $72\% \pm 3.2\%$; HP-β-CD-PEI/siRNA, $77\% \pm 3.2\%$; FA-HP-β-CD-PEI/DOX, $59\% \pm 1.8\%$; FA-HP-β-CD-PEI/siRNA, $65\% \pm 4.6\%$; HP-β-CD-PEI/DOX/siRNA, $47\% \pm 6.3\%$; FA-HP-β-CD-PEI/DOX/siRNA, $28\% \pm 5.6\%$). For HP-β-CD-PEI/DOX and FA-HP-β-CD-PEI/DOX nanocomplexes,
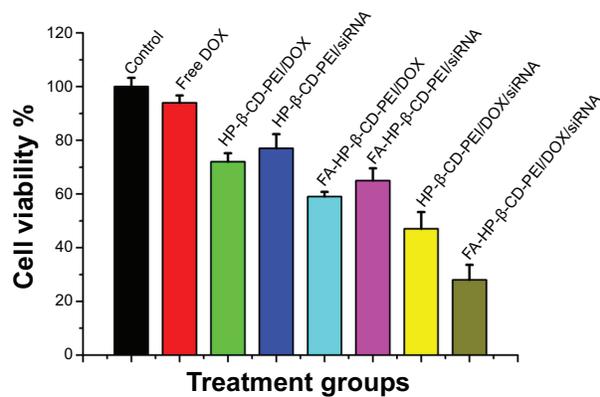
Figure 7 Cell viability of drug-loaded nanocomplexes (HP-β-CD-PEI/DOX, HP-β-CD-PEI/siRNA, FA-HP-β-CD-PEI/DOX, FA-HP-β-CD-PEI/siRNA, HP-β-CD-PEI/DOX/siRNA, and FA-HP-β-CD-PEI/DOX/siRNA).
Notes: Untreated cells and free DOX were controls. Concentrations of DOX and siRNA were 0.5 μg/mL and 100 nM, respectively. Treatment time was 48 hours.
Abbreviations: FA, folic acid; HP-β-CD, hydroxypropyl-β-cyclodextrin; PEI, polyethylenimine; DOX, doxorubicin; siRNA, small interfering RNA.

cell viability was obviously lower than with free DOX treatment, demonstrating that nanocarriers to deliver DOX could improve the pesticide effect of DOX efficiently. For HP-β-CD-PEI/siRNA and FA-HP-β-CD-PEI/siRNA nano-complexes, we also achieved an inhibition of cell prolifera-tion, showing that silencing the *BCL2* gene can inhibit the growth of cancer cells and cause the apoptosis of cancer cells. Comparing all the treatment groups, the FA-HP-β-CD-PEI/DOX/siRNA nanocomplexes showed the best cell apoptosis results (more than 70%), demonstrating the increased efficacy of DOX when combining siRNA *BCL2* gene silencing by a codelivery nanocarrier.

In the FCM cell-apoptosis experiment, the apoptosis kit of annexin V-FITC and PI double staining observed the apoptotic cells, and the apoptosis cells were double stained with annexin V-FITC and PI by FCM. The results are shown in Figure 8 for the treatment groups: free DOX, HP-β-CD-PEI/DOX, HP-β-CD-PEI/siRNA, FA-HP-β-CD-PEI/DOX, FA-HP-β-CD-PEI/siRNA, HP-β-CD-PEI/DOX/siRNA, and FA-HP-β-CD-PEI/DOX/siRNA. In Figure 8, the fluorescence-sign areas of Q2 and Q3 correspond to cell-prophase apoptosis and the cell later-period apoptosis, respectively (the whole apoptosis quantity is Q2 + Q3). The cell-apoptosis quantity increased gradually from the treatment group of free DOX to FA-HP-β-CD-PEI/DOX/siRNA. The concentration of DOX was fixed at 0.5 μg/mL in this experiment, and this concentration resulted in very little MCF-7/Adr cell apoptosis (in the free DOX group, cell apoptosis was almost the same as the control). How-ever, in the FA-HP-β-CD-PEI/DOX/siRNA group (DOX 0.5 μg/mL, siRNA 100 nM), cell apoptosis was about 70%

(45.6%+24.4%): very high cell apoptosis after treating with FA-HP-β-CD-PEI/DOX/siRNA nanocomplexes. Using the FA-HP-β-CD-PEI carrier to codeliver the DOX and the siRNA-BCL2 to the MCF-7/Adr cells can bring a synergistic effect by chemical and gene drugs for overcoming MDR and enhancing cell apoptosis.

Next, to study further the synergistic effect of siRNA and DOX by the codelivery system, the morphology of MCF-7/Adr cells treated with various groups was observed by Bio-TEM. As shown in Figure 9, untreated MCF-7/Adr cells (control) exhibited no morphological changes in the Bio-TEM image. After treatment with free DOX, the MCF-7/Adr cells remained as stretched and polygonal as the control: abundant microvilli were observed on the surface, while plenty of mitochondria were observed in the cells, and the cell membrane and nuclear membrane were still well preserved, with the nucleus containing a nucleolus and euchromatin, because these MCF-7/Adr cells had drug-resistant ability and the concentration of DOX (0.5 μg/mL) had no effect on cell survival. When the cells were incubated with HP-β-CD-PEI/DOX nanocomplexes, Bio-TEM imaging showed that the MCF-7/Adr cells appeared to phagocytose the vesicles. This was the phenomenon of early cell apoptosis, and meant that the DOX contained in the CD of the carrier was useful to escape the drug-resistance mechanism of cancer cells. The phenomenon of early cell apoptosis also appeared in the HP-β-CD-PEI/siRNA group through *BCL2* gene silencing. In the FA-HP-β-CD-PEI/DOX group, the FA made more FA-HP-β-CD-PEI/DOX nanocomplexes enter the MCF-7/Adr cells and caused more cell apoptosis. In Bio-TEM imaging (FA-HP-β-CD-PEI/DOX), phagocytosis of vesicles increased, the cells began to contract, microvilli disappeared, organelles were distorted or lysed, large lipid droplets formed, condensed chromatin was located along the nuclear envelope and a well-defined cell membrane, indicating that the apoptosis of the MCF-7/Adr cells became worse. The same conditions appeared in the FA-HP-β-CD-PEI/siRNA group. Using the drug-delivery system to deliver drugs over-came the MDR to a certain extent. When the MCF-7/Adr cells were incubated with HP-β-CD-PEI/DOX/siRNA and FA-HP-β-CD-PEI/DOX/siRNA nanocomplexes, Bio-TEM imaging showed the worst cell apoptosis: the phagocytose vesicles were filled with whole cells, the nucleus was bro-ken, and the organelle also was broken. In particular, in the FA-HP-β-CD-PEI/DOX/siRNA group, the morphology of cells showed complete splitting, apoptotic bodies appeared, and the nuclear chromosomes were completely broken, showing that using the intracellular targeting drug-delivery
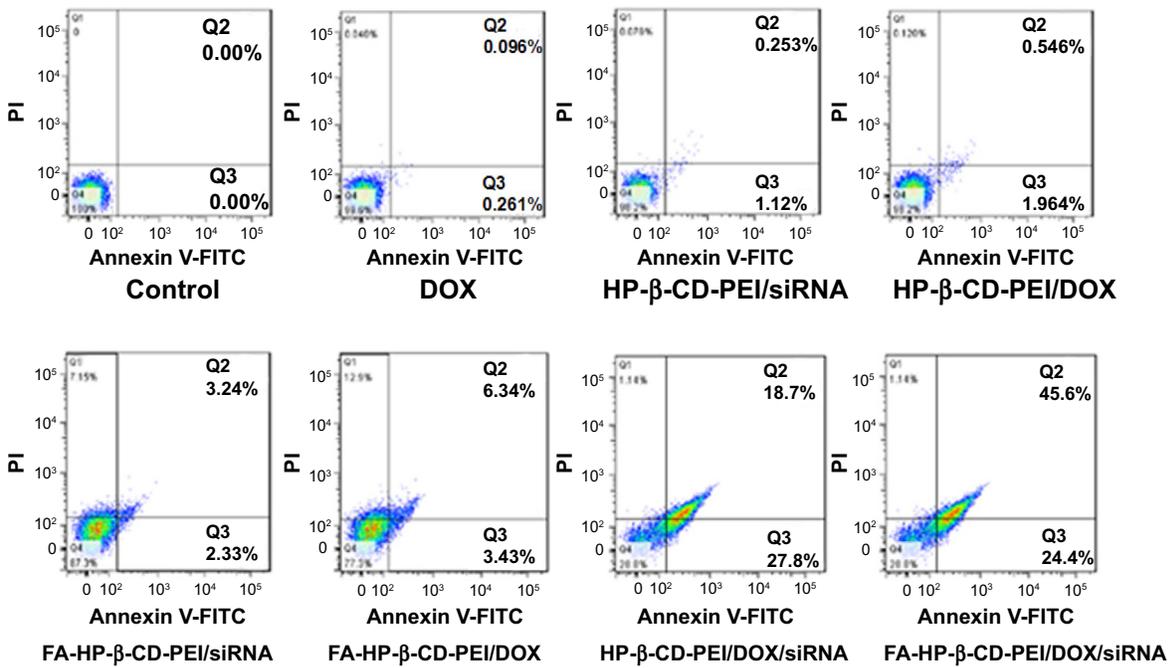
Figure 8 Cell apoptosis of different transportation modalities of a fixed concentration of 0.5 μg/mL of DOX in MCF-7/Adr cells after 48 hours' treatment with differently treated groups.

Notes: The apoptosis of cells was detected by flow cytometry after staining with annexin V-FITC and a PI cell-apoptosis kit; the untreated cell group was used as a control. Cells negative for both annexin V-FITC and PI staining were classified as alive, while cells that stained positive for annexin V-FITC and negative for PI were classified as apoptotic. Cells that stained positive for PI were classified as necrotic. The concentration of BCL2 siRNA used was 100 nM.

Abbreviations: DOX, doxorubicin; FITC, fluorescein isothiocyanate; PI, propidium iodide; FA, folic acid; HP-β-CD, hydroxypropyl-β-cyclodextrin; PEI, polyethylenimine; siRNA, small interfering RNA.
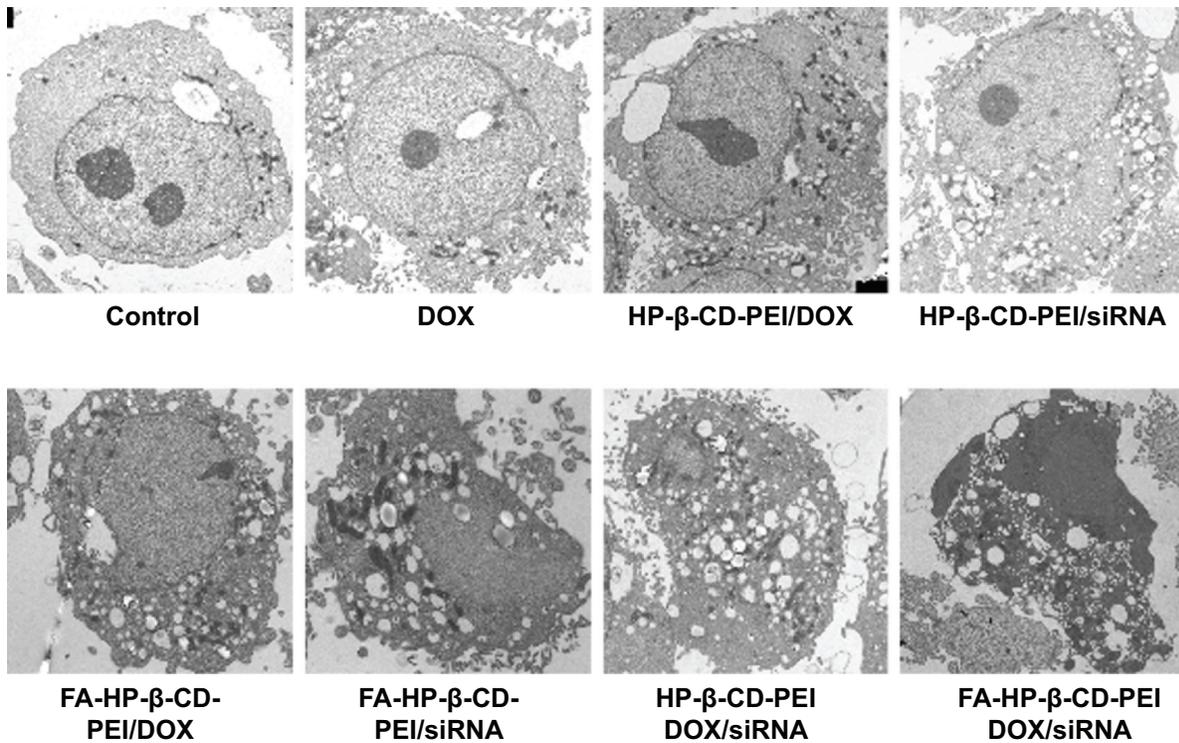
Figure 9 Morphological study of MCF-7/Adr cells after treatment with different modalities for 48 hours by Bio-TEM.

Notes: TEM of MCF-7/Adr cells after treatment with different modalities showed the major ultrastructural changes for each sample. Concentrations of DOX and BCL2 siRNA were 0.5 μg/mL and 100 nM, respectively.

Abbreviations: TEM, transmission electron microscopy; DOX, doxorubicin; siRNA, small interfering RNA; FA, folic acid; HP-β-CD, hydroxypropyl-β-cyclodextrin; PEI, polyethylenimine.

system to codeliver chemical and gene drugs achieved very good synergistic effects to kill MDR cancer cells.

In the cells apoptosis experiments, we achieved a good cell-apoptosis result when using the codelivery drug system to codeliver the DOX and the BCL2 siRNA to MCF-7/Adr cells for apoptosis induction while the concentration of DOX was 0.5 µg/mL. The result from FCM and Bio-TEM, which are consistent with the WB results, demonstrate that this tumor-targeting codelivery system provided a potential platform for combined cancer treatment using chemical and gene drugs simultaneously to overcome MDR in cancer therapy.

Conclusion

We developed a tumor-targeting codelivery nanocarrier (FA-HP-β-CD-PEI) to deliver DOX and siRNA simultaneously with synergistic therapeutics for overcoming MDR. This codelivery nanocarrier displayed a high capability to simultaneously transport DOX and siRNA in MCF-7/Adr cells. Systematic biological experiments revealed that DOX-inducible upregulation of the antiapoptotic *BCL2* gene in MCF-7/Adr cells was significantly suppressed by codelivered BCL2 siRNA. Consequently, MCF-7/Adr cell apoptosis was enhanced, and the potency of DOX in inducing cell death was greatly potentiated through the synergistic effect of the two therapeutic agents with combined therapy. Our study showed the potential of the FA-HP-β-CD-PEI nanocarrier as a tumor-targeting nanoplatform for siRNA and chemical drug codelivery in biomedical applications, and the combination of chemotherapy and gene-therapy technology as a strategy in the treatment of cancer with MDR could be achieved by such codelivery platforms.

Acknowledgments

Disclosure

The authors report no conflicts of interest in this work.

References

1. Jemal A, Bray F, Center MM, Ferlay J, Ward E, Forman D. Global cancer statistics. *CA Cancer J Clin*. 2011;61:69–90.
2. Takara K, Sakaeda T, Okumura K. An update on overcoming MDR1-mediated multidrug resistance in cancer chemotherapy. *Curr Pharm Des*. 2006;12:273–286.
3. Gottesman MM, Fojo T, Bates SE. Multidrug resistance in cancer: role of ATP-dependent transporters. *Nat Rev Cancer*. 2002;2:48–58.
4. McCubrey JA, Steelman LS, Kempf CR, et al. Therapeutic resistance resulting from mutations in Raf/MEK/ERK and PI3K/PTEN/Akt/mTOR signaling pathways. *J Cell Physiol*. 2011;226:2762–2781.
5. Fire A, Xu S, Montgomery MK, Kostas SA, Driver SE, Mello CC. Potent and specific genetic interference by double-stranded RNA in *Caenorhabditis elegans*. *Nature*. 1998;391:806–811.
6. Kim DH, Rossi JJ. Strategies for silencing human disease using RNA interference. *Nat Rev Genet*. 2007;8:173–184.
7. Whitehead KA, Langer R, Anderson DG. Knocking down barriers: advances in siRNA delivery. *Nat Rev Drug Discov*. 2009;8:129–138.
8. Miele E, Spinelli GP, Miele E, et al. Nanoparticle-based delivery of small interfering RNA: challenges for cancer therapy. *Int J Nanomedicine*. 2012;7:3637–3657.
9. Fernandes JC, Qiu X, Winnik FM, et al. Linear polyethylenimine produced by partial acid hydrolysis of poly(2-ethyl-2-oxazoline) for DNA and siRNA delivery in vitro. *Int J Nanomedicine*. 2013;8:4091–4102.
10. Park SC, Nam JP, Kim YM, Kim JH, Nah JW, Jang MK. Branched polyethylenimine-grafted-carboxymethyl chitosan copolymer enhances the delivery of pDNA or siRNA in vitro and in vivo. *Int J Nanomedicine*. 2013;8:3663–3677.
11. Li JM, Wang YY, Zhang W, Su H, Ji LN, Mao ZW. Low-weight polyethylenimine cross-linked 2-hydroxypopyl-ß-cyclodextrin and folic acid as an efficient and nontoxic siRNA carrier for gene silencing and tumor inhibition by VEGF siRNA. *Int J Nanomedicine*. 2013;8:2101–2117.
12. Deng L, Zhang Y, Ma L, et al. Comparison of anti-EGFR-Fab' conjugated immunoliposomes modified with two different conjugation linkers for siRNA delivery in SMMC-7721 cells. *Int J Nanomedicine*. 2013;8:3271–3283.
13. Chen C, Yeh M, Shiau C, Chiang C, Lu D. Efficient downregulation of VEGF in retinal pigment epithelial cells by integrin ligand-labeled liposome-mediated siRNA delivery. *Int J Nanomedicine*. 2013;8: 2613–2627.
14. Malhotra M, Tomaro-Duchesneau C, Saha S, Kahouli I, Prakash S. Development and characterization of chitosan-PEG-TAT nanoparticles for the intracellular delivery of siRNA. *Int J Nanomedicine*. 2013;8: 2041–2052.
15. Fernandes JC, Qiu X, Winnik FM, et al. Low molecular weight chitosan conjugated with folate for siRNA delivery in vitro: optimization studies. *Int J Nanomedicine*. 2012;7:5833–5845.
16. Zhao JJ, Qiu XL, Wang ZP, Pan J, Chen J, Han JS. Application of quantum dots as vectors in targeted survivin gene siRNA delivery. *Int J Nanomedicine*. 2013;6:303–309.
17. Li JM, Zhao MX, Su H, et al. Multifunctional quantum-dot-based siRNA delivery for HPV18 E6 gene silence and intracellular imaging. *Biomaterials*. 2011;32:7978–7987.
18. Zou S, Cao N, Cheng D, et al. Enhanced apoptosis of ovarian cancer cells via nanocarrier-mediated codelivery of siRNA and doxorubicin. *Int J Nanomedicine*. 2012;7:3823–3835.
19. Zhu C, Jung S, Luo S, et al. Co-delivery of siRNA and paclitaxel into cancer cells by biodegradable cationic micelles based on PDMAEMA-PCL-PDMAEMA triblock copolymers. *Biomaterials*. 2010;31: 2408–2416.
20. Saad M, Garbuzenko OB, Minko T. Co-delivery of siRNA and an anti-cancer drug for treatment of multidrug-resistant cancer. *Nanomedicine (Lond)*. 2008;3:761–776.
21. Chen AM, Zhang M, Wei D, et al. Co-delivery of doxorubicin and Bcl-2 siRNA by mesoporous silica nanoparticles enhances the efficacy of chemotherapy in multidrug-resistant cancer cells. *Small*. 2009;5: 2673–2677.
22. Xiao Y, Jaskula-Sztul R, Javadi A, et al. Co-delivery of doxorubicin and siRNA using octreotide-conjugated gold nanorods for targeted neuroendocrine cancer therapy. *Nanoscale*. 2012;4:7185–7193.
23. Li JM, Wang YY, Zhao MX, et al. Multifunctional QD-based co-delivery of siRNA and doxorubicin to HeLa cells for reversal of multidrug resistance and real-time tracking. *Biomaterials*. 2012;33:2780–2790.

24. Godbey WT, Wu KK, Mikos AG. Poly(ethylenimine) and its role in gene delivery. *J Control Release*. 1999;60:149–160.

25. Boussif O, Lezoualc'h F, Zanta MA, et al. A versatile vector for gene and oligonucleotide transfer into cells in culture and in vivo: polyethylenimine. *Proc Natl Acad Sci U S A*. 1995;92:7297–7301.

26. Mintzer MA, Simanek EE. Nonviral vectors for gene delivery. *Chem Rev*. 2009;109:259–302.

27. Kunath K, von Harpe A, Fischer D, et al. Low-molecular-weight polyethylenimine as a non-viral vector for DNA delivery: comparison of physicochemical properties, transfection efficiency and in vivo distribution with high-molecular-weight polyethylenimine. *J Control Release*. 2003;89:113–125.

28. Kim YH, Park JH, Lee M, Park TG, Kim SW. Polyethylenimine with acid-labile linkages as a biodegradable gene carrier. *J Control Release*. 2005;103:209–219.

29. Ping Y, Liu C, Zhang Z, Liu KL, Chen J, Li J. Chitosan-graft-(PEI-β-cyclodextrin) copolymers and their supramolecular PEGylation for DNA and siRNA delivery. *Biomaterials*. 2011;32:8328–8341.

30. Yao H, Ng SS, Tucker WO, et al. The gene transfection efficiency of a folate-PEI600-cyclodextrin nanopolymer. *Biomaterials*. 2009;30: 5793–5803.

31. Davis ME, Brewster ME. Cyclodextrin-based pharmaceutics: past, present and future. *Nat Rev Drug Discov*. 2004;3:1023–1035.

32. Li J, Loh XJ. Cyclodextrin-based supramolecular architectures: syntheses, structures, and applications for drug and gene delivery. *Adv Drug Deliv Rev*. 2008;60:1000–1017.

33. Brewster ME, Hora MS, Simpkins JW, Bodor N. Use of 2-hydroxypropyl-beta-cyclodextrin as a solubilizing and stabilizing excipient for protein drugs. *Pharm Res*. 1991;8:792–795.

34. Gould S, Scott RC. 2-Hydroxypropyl-beta-cyclodextrin (HP-beta-CD): a toxicology review. *Food Chem Toxicol*. 2005;43:1451–1459.

35. Domańska U, Pelczarska A, Pobudkowska A. Effect of 2-hydroxypropyl-β-cyclodextrin on solubility of sparingly soluble drug derivatives of anthranilic acid. *Int J Mol Sci*. 2011;12:2383–2394.

36. Zhou JW, Ritter H. Cyclodextrin functionalized polymers as drug delivery systems. *Polym Chem*. 2010;1:1552–1559.

37. Heidel JD, Schluep T. Cyclodextrin-containing polymers: versatile platforms of drug delivery materials. *J Drug Deliv*. 2012;2012:262731.

38. Heidel JD. Linear cyclodextrin-containing polymers and their use as delivery agents. *Expert Opin Drug Deliv*. 2006;3:641–646.

39. Brannon-Peppas L, Blanchette JO. Nanoparticle and targeted systems for cancer therapy. *Adv Drug Deliv Rev*. 2004;56:1649–1659.

40. Sudimack J, Lee RJ. Targeted drug delivery via the folate receptor. *Adv Drug Deliv Rev*. 2000;41:147–162.

41. Win KY, Feng SS. Effects of particle size and surface coating on cellular uptake of polymeric nanoparticles for oral delivery of anticancer drugs. *Biomaterials.* 2005;26:2713–2722.

42. He C, Hu Y, Yin L, Tang C, Yin C. Effects of particle size and surface charge on cellular uptake and biodistribution of polymeric nanoparticles. *Biomaterials*. 2010;31:3657–3666.

43. Liu D, Mori A, Huang L. Role of liposome size and RES blockade in controlling biodistribution and tumor uptake of GM1-containing liposomes. *Biochim Biophys Acta*. 1992;1104:95–101.

44. Uekama K, Hirayama F, Irie T. Cyclodextrin drug carrier systems. *Chem Rev*. 1998;98:2045–2076.

45. Decaudin D, Geley S, Hirsch T, et al. Bcl-2 and Bcl-XL antagonize the mitochondrial dysfunction preceding nuclear apoptosis induced by chemotherapeutic agents. *Cancer Res*. 1997;57:62–67.

Supplementary materials

Table S1 Properties of carriers and DOX-loaded carriers

	DLS diameter	PDI	Zeta potential	Loading content of DOX
HP-β-CD-PEI/DOX	312.5±5.2	0.166	28.6±1.7	12.6 wt%
FA-HP-β-CD-PEI/DOX	352.6±2.3	0.174	21.4±2.3	11.5 wt%
HP-β-CD-PEI/DOX/siRNA	271.5±3.6	0.215	18.7±1.5	–
FA-HP-β-CD-PEI/DOX/siRNA	297.4±1.7	0.137	13.5±1.9	–

Abbreviations: DOX, doxorubicin; DLS, dynamic light scattering; PDI, polydispersity index; siRNA, small interfering RNA; FA, folic acid; HP-β-CD, hydroxypropyl-β-cyclodextrin; PEI, polyethylenimine.
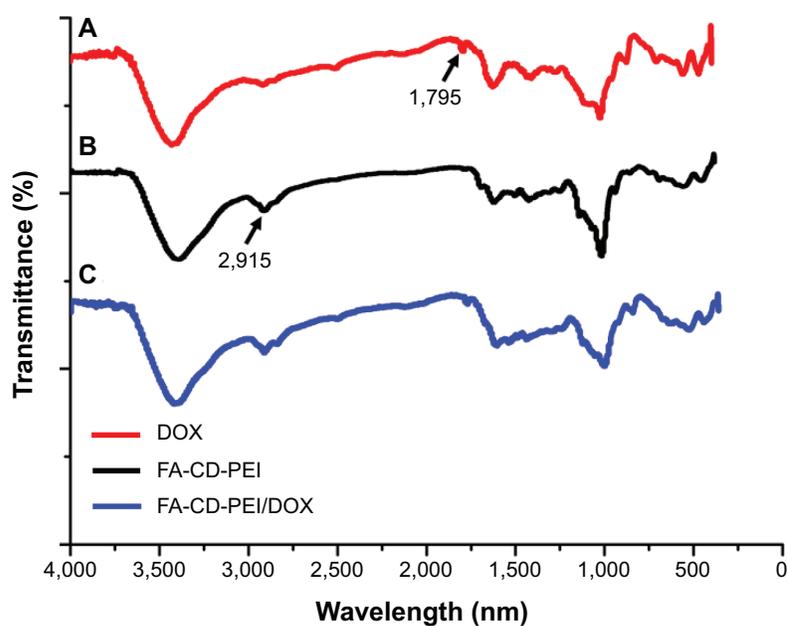
Figure S1 FTIR spectra of DOX (**A**), FA-HP-β-CD-PEI nanocarriers (**B**), and FA-HP-β-CD-PEI/DOX nanocomplexes (**C**).
Abbreviations: FTIR, Fourier-transform infrared; DOX, doxorubicin; FA, folic acid; HP-β-CD, hydroxypropyl-β-cyclodextrin; PEI, polyethylenimine.
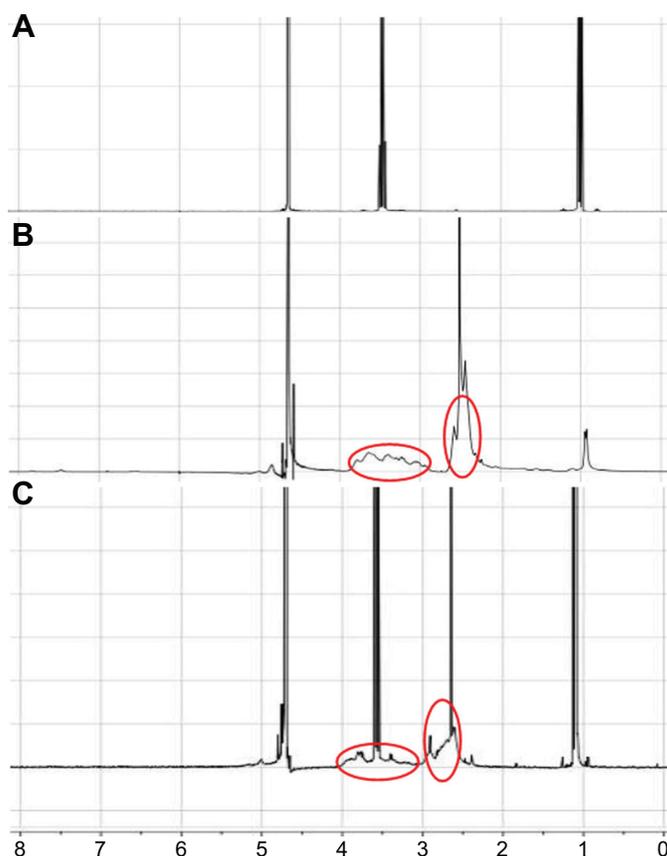
Figure S2 ^{1}H NMR spectra of DOX (**A**), FA-HP-β-CD-PEI nanocarriers (**B**), and FA-HP-β-CD-PEI/DOX nanocomplexes (**C**).
Abbreviations: NMR, nuclear magnetic resonance; DOX, doxorubicin; FA, folic acid; HP-β-CD, hydroxypropyl-β-cyclodextrin; PEI, polyethylenimine.
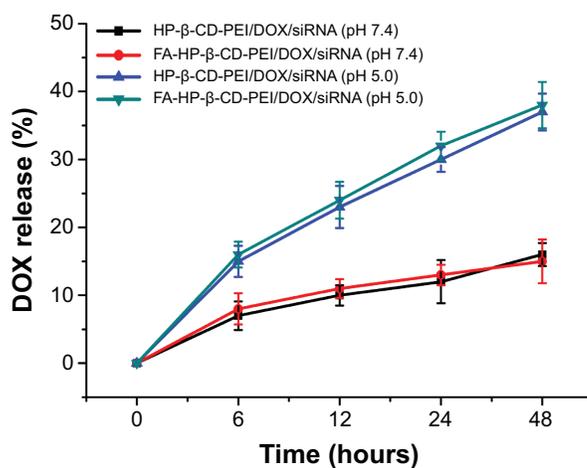

Figure S3 The DOX release behavior of nanocarrier/DOX/siRNA nanocomplexes in different pH conditions (pH 5.0 and pH 7.4).
Notes: The siRNA binding with DOX-loaded nanocomplexes had no effect on DOX-release behavior. DOX concentration of 0.5 μg/mL, siRNA concentration of 100 nM.
Abbreviations: DOX, doxorubicin; siRNA, small interfering RNA; FA, folic acid; HP-β-CD, hydroxypropyl-β-cyclodextrin; PEI, polyethylenimine.